Chapter 5 Failure Analysis

In the past several chapters the influences of geometry and orthotropy on the responses of elliptical and circular cylinders constructed with quasi-isotropic, axially-stiff, and circumferentially-stiff laminates have been evaluated. Both geometrically linear and nonlinear analyses have been used. In this chapter, an evaluation of failure using the maximum stress and Hashin [7] failure criteria is presented for elliptical cylinders by considering geometrically linear and nonlinear analyses and quasi-isotropic, axially-stiff, and circumferentially-stiff laminates. The failure criteria are used to assess the mode of failure (e.g., tensile or compressive fiber or matrix modes), the location of failure, and the pressure at failure.

5.1 Failure Criteria

The maximum stress and Hashin failure criteria are three-dimensional theories that are based on one-dimensional uniaxial and shear failure stresses. The one-dimensional failure stresses are denoted as follows:

σ_A^+ = tensile failure stress in the fiber direction

σ_A^- = compressive failure stress in the fiber direction (absolute value)

σ_T^+ = tensile failure stress transverse to the fiber direction

σ_T^- = compressive failure stress transverse to the fiber direction (absolute value)

τ_T = transverse failure shear stress

τ_A = axial failure shear stress

For graphite-epoxy typical values of the failure stresses are [2]:

$$
\begin{aligned}
\sigma_A^+ &= 200,000 \text{ psi} \\
\sigma_A^- &= 180,000 \text{ psi} \\
\sigma_T^+ &= 7250 \text{ psi} \\
\sigma_T^- &= 29,000 \text{ psi} \\
\tau_A &= 14,500 \text{ psi} \\
\tau_T &= 14,500 \text{ psi}
\end{aligned}
\tag{5.1}
$$

The maximum stress and Hashin failure criteria are linear and quadratic in the stresses, respectively. For the maximum stress criterion, failure is assumed to occur when any one of the stresses in the principal material coordinate system equals the respective failure stress level. For the Hashin criterion, the stresses in the principal material coordinate system and the failure stresses are combined quadratically to form a number of expressions and the material is assumed to fail when any one of the expressions terms reaches unity. Alternatively, the maximum stress criterion can be formatted so that failure is assumed to occur when the ratio of any one of the stresses in the principal material system divided by the respective failure stress level reaches unity. Therefore, these two criteria can be put on a somewhat similar basis.

5.1.1 Maximum Stress Theory

For the maximum stress criterion, there are three modes of failure: tensile, compressive, and shear. There is assumed to be no interaction between modes of failure or between the stresses in principal material coordinate system. For example, tensile failure occurs when either σ_{11} or σ_{22} reaches the respective failure value, but σ_{22} doesn't interact with σ_{11} to cause tensile failure, say, when both are 90% of their failure value. The shear failure mode is independent of sign, such that a negative or a positive shear stress is equally capable of causing shear failure. The failure modes of the maximum stress theory are denoted as follows:

Tensile Modes (σ_{11}, $\sigma_{22} > 0$):

$$\sigma_{11} < \sigma_A^+ \qquad \sigma_{22} < \sigma_T^+ \tag{5.2}$$

Compressive Modes (σ_{11}, $\sigma_{22} < 0$):

$$-\sigma_{11} < \sigma_A^- \qquad -\sigma_{22} < \sigma_T^- \tag{5.3}$$

Shear Modes:

$$|\sigma_{23}| < \tau_T \qquad |\sigma_{13}| < \tau_A \qquad |\sigma_{12}| < \tau_A \tag{5.4}$$

For the purpose of computation, the following is a more convenient form for the maximum stress criterion:

Tensile Modes (σ_{11}, $\sigma_{22} > 0$):

$$\frac{\sigma_{11}}{\sigma_A^+} < 1 \qquad \frac{\sigma_{22}}{\sigma_T^+} < 1 \tag{5.5}$$

Compressive Modes (σ_{11}, $\sigma_{22} < 0$):

$$\frac{-\sigma_{11}}{\sigma_A^-} < 1 \qquad \frac{-\sigma_{22}}{\sigma_T^-} < 1 \tag{5.6}$$

Shear Modes:

$$\frac{|\sigma_{23}|}{\tau_T} < 1 \qquad \frac{|\sigma_{13}|}{\tau_A} < 1 \qquad \frac{|\sigma_{12}|}{\tau_A} < 1 \tag{5.7}$$

With this form of the failure criterion, the cylinder is assumed to be safe from failure if all seven of the left hand sides of eqs. 5.5-5.7 are less than unity, and failure is assumed to occur when any one of the seven left hand sides equals unity.

5.1.2 Hashin Theory

For the Hashin criterion, there are four modes of failure: tensile fiber, compressive fiber, tensile matrix, and compressive matrix. The Hashin theory is written in terms of quadratic stress

polynomials such that the interaction between the stresses represents an average stress state. The four modes of the Hashin criterion are denoted as follows:

Tensile Fiber Mode: $\sigma_{11} > 0$

$$\left(\frac{\sigma_{11}}{\sigma_A^+}\right)^2 + \frac{1}{\tau_A^2}(\sigma_{12}^2 + \sigma_{13}^2) < 1 \tag{5.8}$$

Compressive Fiber Mode: $\sigma_{11} < 0$

$$\frac{-\sigma_{11}}{\sigma_A^-} < 1 \tag{5.9}$$

Tensile Matrix Mode: $(\sigma_{22} + \sigma_{33}) > 0$

$$\frac{1}{(\sigma_T^+)^2}(\sigma_{22} + \sigma_{33})^2 + \frac{1}{\tau_T^2}(\sigma_{23}^2 - \sigma_{22}\sigma_{33}) + \frac{1}{\tau_A^2}(\sigma_{12}^2 + \sigma_{13}^2) < 1 \tag{5.10}$$

Compressive Matrix Mode: $(\sigma_{22} + \sigma_{33}) < 0$

$$\frac{1}{\sigma_T^-}\left[\left(\frac{\sigma_T^-}{2\tau_T}\right)^2 - 1\right](\sigma_{22} + \sigma_{33}) + \frac{1}{4\tau_T^2}(\sigma_{22} + \sigma_{33})^2 + \frac{1}{\tau_T^2}(\sigma_{23}^2 - \sigma_{22}\sigma_{33}) + \frac{1}{\tau_A^2}(\sigma_{12}^2 + \sigma_{13}^2) < 1 \tag{5.11}$$

However, since σ_{33} is assumed to be negligible for the present analysis of the elliptical cylinders, the Hashin failure criterion simplifies as follows:

Tensile Fiber Mode: $\sigma_{11} > 0$

$$\left(\frac{\sigma_{11}}{\sigma_A^+}\right)^2 + \frac{1}{\tau_A^2}(\sigma_{12}^2 + \sigma_{13}^2) < 1 \tag{5.12}$$

Compressive Fiber Mode: $\sigma_{11} < 0$

$$\frac{-\sigma_{11}}{\sigma_A^-} < 1 \tag{5.13}$$

Tensile Matrix Mode: $\sigma_{22} > 0$

$$\left(\frac{\sigma_{22}}{\sigma_T^+}\right)^2 + \left(\frac{\sigma_{23}}{\tau_T}\right)^2 + \frac{1}{\tau_A^2}(\sigma_{12}^2 + \sigma_{13}^2) < 1 \tag{5.14}$$

Compressive Matrix Mode: $\sigma_{22} < 0$

$$\frac{\sigma_{22}}{\sigma_T^-}\left[\left(\frac{\sigma_T^-}{2\tau_T}\right)^2 - 1\right] + \left(\frac{\sigma_{22}}{2\tau_T}\right)^2 + \left(\frac{\sigma_{23}}{\tau_T}\right)^2 + \frac{1}{\tau_A^2}(\sigma_{12}^2 + \sigma_{13}^2) < 1 \tag{5.15}$$

Hence, the cylinder is assumed to be safe from failure when all four left hand sides of eqs. 5.12-5.15 are less than unity, and failure is assumed to have occurred when any one of the four left hand sides equals unity.

5.2 Determination of Stresses

In order to make use of either failure criterion, computation of the inplane and interlaminar shear stresses in the principal material coordinate system, which is shown in fig. 5-1, are necessary. Note the coordinate ξ_3 coincides with the through-thickness coordinate ζ, where ζ varies from $-H/2 \le \zeta \le H/2$ and is zero at the wall midsurface, or reference surface. The normal and shear stresses in the (ξ_1,ξ_2) plane $(\sigma_1, \sigma_2, \sigma_{12})$ are termed inplane stresses. The shear stresses trans-

verse, or perpendicular, to the (ξ_1,ξ_2) plane (σ_{13}, σ_{23}) are called interlaminar stresses. (Actually due to the complementary nature of shear stresses, σ_{13} and σ_{23} also act parallel to the 1-2 plane)

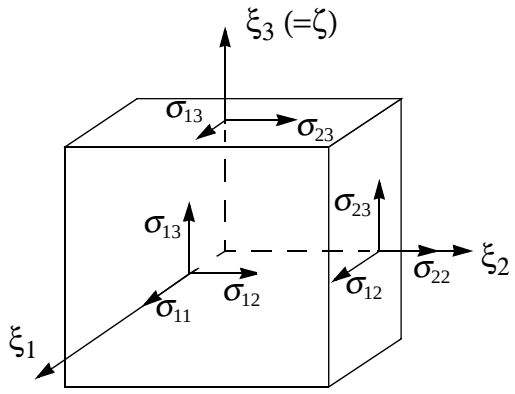

Figure 5-1. Inplane and interlaminar stresses in principal material direction.

5.2.1 Inplane Stresses

The inplane stresses can be written in terms of reference surface strains and curvatures, which are, as seen in previous chapters, a direct result of the semi-analytical solution. These stresses vary through the thickness of the cylinder wall and the inplane stresses in the k^{th} layer are given by

$$\begin{bmatrix}\sigma_x\\ \sigma_s\\ \tau_{xs}\end{bmatrix}^k = \begin{bmatrix}\overline{Q}_{11} & \overline{Q}_{12} & \overline{Q}_{16}\\ \overline{Q}_{12} & \overline{Q}_{22} & \overline{Q}_{26}\\ \overline{Q}_{16} & \overline{Q}_{26} & \overline{Q}_{66}\end{bmatrix}^k \begin{bmatrix}\varepsilon_x\\ \varepsilon_s\\ \gamma_{xs}\end{bmatrix}^k = \begin{bmatrix}\overline{Q}_{11} & \overline{Q}_{12} & \overline{Q}_{16}\\ \overline{Q}_{12} & \overline{Q}_{22} & \overline{Q}_{26}\\ \overline{Q}_{16} & \overline{Q}_{26} & \overline{Q}_{66}\end{bmatrix}^k \begin{bmatrix}\varepsilon_x^o + \zeta\kappa_x^o\\ \varepsilon_s^o + \zeta\kappa_s^o\\ \gamma_{xs}^o + \zeta\kappa_{xs}^o\end{bmatrix}, \tag{5.16}$$

where $[\overline{Q}_{ij}]^k$ is the transformed reduced stiffness matrix of the k^{th} layer, and eq. 1.6 has been employed to compute the strains in the k^{th} layer. The stresses in principal material coordinate system can be obtained by transformation, namely

$$\begin{bmatrix}\sigma_1\\ \sigma_2\\ \sigma_{12}\end{bmatrix}^k = \begin{bmatrix} cos^2\theta_k & sin^2\theta_k & 2cos\theta_k sin\theta_k \\ sin^2\theta_k & cos^2\theta_k & -2cos\theta_k sin\theta_k \\ -cos\theta_k sin\theta_k & cos\theta_k sin\theta_k & (cos^2\theta_k - sin^2\theta_k)\end{bmatrix}\begin{bmatrix}\sigma_x\\ \sigma_s\\ \tau_{xs}\end{bmatrix}^k, \tag{5.17}$$

where θ_k is the fiber angle of the k^{th} layer with respect to the axial direction of the cylinder.

5.2.2 Interlaminar Stresses

For the geometrically linear case, the interlaminar stresses in the layers, τ_{rs} and τ_{rx}, can be evaluated by using the equilibrium equations of linear elasticity written in a cylinder coordinate system, namely,

$$\begin{aligned}\frac{\partial\sigma_r}{\partial r} + \frac{\partial\tau_{rs}}{\partial s} + \frac{\partial\tau_{rx}}{\partial x} + \frac{\sigma_r - \sigma_s}{r} &= 0\\ \frac{\partial\sigma_s}{\partial s} + \frac{\partial\tau_{rs}}{\partial r} + \frac{\partial\tau_{xs}}{\partial x} + \frac{2}{r}\tau_{rs} &= 0\\ \frac{\partial\sigma_x}{\partial x} + \frac{\partial\tau_{rx}}{\partial r} + \frac{\partial\tau_{xs}}{\partial s} + \frac{1}{r}\tau_{rx} &= 0,\end{aligned} \tag{5.18}$$

where the *r*, *x*, and *s* coordinates are shown in detail in fig. 5-2. In fig. 5-2 both *r*-*s* and *r*-*x* cylinder wall cross sections are shown. The radius of curvature of an arbitrary point within the wall is *r* and, recall, the radius of curvature of the wall midsurface is *R*(*s*). (The equilibrium equations of linear elasticity are used because, as will be shown, the contributions of the interlaminar stresses to either failure criteria considered are quite small. It therefore was concluded that the interlaminar stresses were not causing failure. The nonlinear equations of equilibrium are very complex

and could not be treated in the manner of the section to follow to compute τ_{rs} and τ_{rx} as a function of r.)

Figure 5-2. Geometry of a section of the cylinder wall.

In order to determine τ_{rx}, eq. 5.18c is rewritten as follows:

$$\frac{\partial \tau_{rx}}{\partial r} + \frac{1}{r}\tau_{rx} = \frac{1}{r}\frac{\partial}{\partial r}(r\tau_{rx}) = -\left(\frac{\partial \sigma_x}{\partial x} + \frac{\partial \tau_{xs}}{\partial s}\right) \quad . \tag{5.19}$$

Defining

$$r = R(s) + \zeta \, , \tag{5.20}$$

it follows that

$$\frac{\partial}{\partial r} = \frac{\partial}{\partial \zeta} \tag{5.21}$$

so eq. 5.19 becomes

$$\frac{\partial}{\partial \zeta}[(R(s) + \zeta)\tau_{rx}] = -\left(\frac{\partial \sigma_x}{\partial x} + \frac{\partial \tau_{xs}}{\partial s}\right)(R(s) + \zeta) \, . \tag{5.22}$$

Before $\frac{\partial}{\partial \zeta}[(R(s) + \zeta)\tau_{rx}]$ can be integrated with respect to ζ to obtain τ_{rx}, σ_x and τ_{xs} need to be written explicitly in terms of ζ, namely, from eq. 5.16, as

$$\begin{aligned} \sigma_x &= \overline{Q}_{11}(\varepsilon_x^o + \zeta\kappa_x^o) + \overline{Q}_{12}(\varepsilon_s^o + \zeta\kappa_s^o) + \overline{Q}_{16}(\gamma_{xs}^o + \zeta\kappa_{xs}^o) = \sigma_x^\varepsilon + \zeta\sigma_x^\kappa \\ \tau_{xs} &= \overline{Q}_{16}(\varepsilon_x^o + \zeta\kappa_x^o) + \overline{Q}_{26}(\varepsilon_s^o + \zeta\kappa_s^o) + \overline{Q}_{66}(\gamma_{xs}^o + \zeta\kappa_{xs}^o) = \tau_{xs}^\varepsilon + \zeta\tau_{xs}^\kappa \end{aligned} \tag{5.23}$$

where,

$$\begin{aligned}
\sigma_x^{\varepsilon} &= \bar{Q}_{11}\varepsilon_x^o + \bar{Q}_{12}\varepsilon_s^o + \bar{Q}_{16}\gamma_{xs}^o \\
\sigma_x^{\kappa} &= \bar{Q}_{11}\kappa_x^o + \bar{Q}_{12}\kappa_s^o + \bar{Q}_{16}\kappa_{xs}^o \\
\tau_{xs}^{\varepsilon} &= \bar{Q}_{16}\varepsilon_x^o + \bar{Q}_{26}\varepsilon_s^o + \bar{Q}_{66}\gamma_{xs}^o \\
\tau_{xs}^{\kappa} &= \bar{Q}_{16}\kappa_x^o + \bar{Q}_{26}\kappa_s^o + \bar{Q}_{66}\kappa_{xs}^o .
\end{aligned} \tag{5.24}$$

Within a layer these quantities do not vary with the thickness coordinate, ζ. Equation 5.22 can now be written as,

$$\begin{aligned}
\frac{\partial}{\partial\zeta}[(R(s)+\zeta)\tau_{rx}] &= -\left(\frac{\partial\sigma_x^{\varepsilon}}{\partial x} + \zeta\frac{\partial\sigma_x^{\kappa}}{\partial x} + \frac{\partial\tau_{xs}^{\varepsilon}}{\partial s} + \zeta\frac{\partial\tau_{xs}^{\kappa}}{\partial s}\right)(R(s)+\zeta) \\
&= -\left\{\left(\frac{\partial\sigma_x^{\varepsilon}}{\partial x} + \frac{\partial\tau_{xs}^{\varepsilon}}{\partial s}\right)(R(s)+\zeta) + \left(\frac{\partial\sigma_x^{\kappa}}{\partial x} + \frac{\partial\tau_{xs}^{\kappa}}{\partial s}\right)(R(s)\zeta + \zeta^2)\right\}.
\end{aligned} \tag{5.25}$$

Equation 5.25 can be integrated with respect to ζ to obtain

$$(R(s)+\zeta)\tau_{rx} = \hat{h}_x(x,s) - \left\{\left(\frac{\partial\sigma_x^{\varepsilon}}{\partial x} + \frac{\partial\tau_{xs}^{\varepsilon}}{\partial s}\right)\left(R(s)\zeta + \frac{\zeta^2}{2}\right) + \left(\frac{\partial\sigma_x^{\kappa}}{\partial x} + \frac{\partial\tau_{xs}^{\kappa}}{\partial s}\right)\left(R(s)\frac{\zeta^2}{2} + \frac{\zeta^3}{3}\right)\right\}, \tag{5.26}$$

where $\hat{h}_x(x,s)$ is an unknown but to-be-determined function of integration. Dividing eq. 5.26 by $(R(s)+\zeta)$ yields

$$\tau_{rx} = \frac{\hat{h}_x(x,s)}{R(s)+\zeta} - \left\{\left(\frac{\partial\sigma_x^{\varepsilon}}{\partial x} + \frac{\partial\tau_{xs}^{\varepsilon}}{\partial s}\right)\left[\frac{\left(R(s)+\frac{\zeta}{2}\right)\zeta}{(R(s)+\zeta)}\right] + \left(\frac{\partial\sigma_x^{\kappa}}{\partial x} + \frac{\partial\tau_{xs}^{\kappa}}{\partial s}\right)\left[\frac{\left(R(s)+\frac{2}{3}\zeta\right)\frac{\zeta^2}{2}}{(R(s)+\zeta)}\right]\right\}. \tag{5.27}$$

The terms in square brackets in eq. 5.27 can be simplified. In general, for thin-walled cylinders ζ is small when compared to *R(s)*. This can be shown as follows:

$$\frac{\zeta}{R(s)} < \frac{\zeta_{MAX}}{R_{MIN}} = \frac{1}{2e^2}\left(\frac{H}{a}\right) = \frac{1}{2(0.7)^2}\left(\frac{0.0495}{5}\right) = 0.0101 \ll 1 \tag{5.28}$$

where the numbers for a nine-layer elliptical cylinder have been used. Therefore,

$$\frac{\zeta}{\mathrm{R}(s)} \ll 1 . \tag{5.29}$$

Thus, for example, the denominator of the terms in eq. 5.27 are

$$(R(s) + \zeta) = R(s)\left(1 + \frac{\zeta}{R(s)}\right) \approx R(s) . \tag{5.30}$$

Using similar arguments on other terms in eq. 5.27, it is concluded that

$$\frac{\left(R(s) + \frac{\zeta}{2}\right)}{(R(s) + \zeta)} \approx 1 \qquad \frac{\left(R(s) + \frac{2}{3}\zeta\right)}{(R(s) + \zeta)} \approx 1. \tag{5.31}$$

Therefore, eq. 5.27 can be reduced to

$$\begin{aligned} \tau_{rx} &= \frac{\hat{h}_x(x, s)}{\mathrm{R(s)}} - \left\{\left(\frac{\partial \sigma_x^{\varepsilon}}{\partial x} + \frac{\partial \tau_{xs}^{\varepsilon}}{\partial s}\right)\zeta + \left(\frac{\partial \sigma_x^{\kappa}}{\partial x} + \frac{\partial \tau_{xs}^{\kappa}}{\partial s}\right)\frac{\zeta^2}{2}\right\} \\ &= h_x(x, s) - \left\{f_x(x, s)\zeta + g_x(x, s)\frac{\zeta^2}{2}\right\}, \end{aligned} \tag{5.32}$$

where $f_x(x,s)$ and $g_x(x,s)$ are known for each layer at a given value of x and s. The unknown function of integration term has been redefined to be $h_x(x,s)$. The function $h_x^{(k)}(x,s)$ for the k^{th} layer can be determined by utilizing the condition that

$$\tau_{\mathrm{rx}} = 0 \text{ at } \zeta = -\frac{\mathrm{H}}{2} \qquad \left(\text{i. e. , } \tau_{rx}^{(1)} = 0 \text{ at } \zeta = -\frac{\mathrm{H}}{2}\right) \tag{5.33}$$

and the continuity condition

$$\tau_{rx}^{(k-1)} = \tau_{rx}^{(k)} , \tag{5.34}$$

where k denotes the layer number. These conditions translate into, respectively,

$$\tau_{rx}^{(1)} = 0 = h_x^{(1)}(x, s) - \left\{f_x^{(1)}(x, s)\left(-\frac{\mathrm{H}}{2}\right) + g_x^{(1)}(x, s)\frac{1}{2}\left(-\frac{\mathrm{H}}{2}\right)^2\right\} \tag{5.35}$$

or

$$h_x^{(1)}(x, s) = \left\{ f_x^{(1)}(x, s)\left(-\frac{\mathrm{H}}{2}\right) + g_x^{(1)}(x, s)\frac{1}{2}\left(-\frac{\mathrm{H}}{2}\right)^2 \right\} \tag{5.36}$$

and

$$h_x^{(k-1)}(x, s) - \left\{ f_x^{(k-1)}(x, s)\zeta_k + g_x^{(k-1)}(x, s)\frac{\zeta_k^2}{2} \right\} = h_x^{(k)}(x, s) - \left\{ f_x^{(k)}(x, s)\zeta_k + g_x^{(k)}(x, s)\frac{\zeta_k^2}{2} \right\} \tag{5.37}$$

or

$$h_x^{(k)}(x, s) = h_x^{(k-1)}(x, s) + (f_x^{(k)}(x, s) - f_x^{(k-1)}(x, s))\zeta_k + (g_x^{(k)}(x, s) - g_x^{(k-1)}(x, s))\frac{\zeta_k^2}{2}, \tag{5.38}$$

for k = 2, 3, ..., n, where n is the total number of layers. The quantity ζ_k is the interfacial location between the k^{th} and $(k\text{-}1)^{st}$ layers.

In order to determine τ_{rs}, eq. 5.18b is rewritten as follows:

$$\frac{\partial \tau_{rs}}{\partial r} + \frac{2}{r}\tau_{rs} = \frac{1}{r^2}\left[\frac{\partial}{\partial \mathrm{r}}(r^2 \tau_{rs})\right] = -\left(\frac{\partial \sigma_s}{\partial s} + \frac{\partial \tau_{xs}}{\partial x}\right). \tag{5.39}$$

Using eq. 5.20 and eq. 5.21, eq. 5.39 becomes

$$\frac{\partial}{\partial \zeta}[(R(s) + \zeta)^2 \tau_{rs}] = -\left(\frac{\partial \sigma_s}{\partial s} + \frac{\partial \tau_{xs}}{\partial x}\right)(R(s) + \zeta)^2 \ . \tag{5.40}$$

Before $\frac{\partial}{\partial \zeta}[(R(s) + \zeta)^2 \tau_{rs}]$ can be integrated with respect to ζ to obtain τ_{rs}, σ_s needs to be written explicitly in terms of ζ, namely, from eq. 5.16, as

$$\sigma_s = \overline{Q}_{12}(\varepsilon_x^o + \zeta\kappa_x^o) + \overline{Q}_{22}(\varepsilon_s^o + \zeta\kappa_s^o) + \overline{Q}_{26}(\gamma_{xs}^o + \zeta\kappa_{xs}^o) = \sigma_s^{\varepsilon} + \zeta\sigma_s^{\kappa} \tag{5.41}$$

where,

$$\sigma_s^{\varepsilon} = \bar{Q}_{12}\varepsilon_x^o + \bar{Q}_{22}\varepsilon_s^o + \bar{Q}_{26}\gamma_{xs}^o$$
$$\sigma_s^{\kappa} = \bar{Q}_{12}\kappa_x^o + \bar{Q}_{22}\kappa_s^o + \bar{Q}_{26}\kappa_{xs}^o. \tag{5.42}$$

Within a layer these quantities do not vary with the thickness coordinate, ζ. Equation 5.40 can now be written as,

$$\frac{\partial}{\partial\zeta}[(R(s)+\zeta)^2\tau_{rs}] = -\left(\frac{\partial\sigma_s^{\varepsilon}}{\partial s} + \zeta\frac{\partial\sigma_s^{\kappa}}{\partial s} + \frac{\partial\tau_{xs}^{\varepsilon}}{\partial x} + \zeta\frac{\partial\tau_{xs}^{\kappa}}{\partial x}\right)(R(s)+\zeta)^2$$
$$= -\left\{\left(\frac{\partial\sigma_s^{\varepsilon}}{\partial s} + \frac{\partial\tau_{xs}^{\varepsilon}}{\partial x}\right)(R(s)+\zeta)^2 + \left(\frac{\partial\sigma_s^{\kappa}}{\partial s} + \frac{\partial\tau_{xs}^{\kappa}}{\partial x}\right)\zeta(R(s)+\zeta)^2\right\}. \tag{5.43}$$

Equation 5.43 can be integrated with respect to ζ to obtain

$$(R(s)+\zeta)^2\tau_{rs} = \hat{h}_s(x,s) -$$
$$\left\{\left(\frac{\partial\sigma_x^{\varepsilon}}{\partial x} + \frac{\partial\tau_{xs}^{\varepsilon}}{\partial s}\right)\left(\zeta R^2(s) + \zeta^2 R(s) + \frac{\zeta^3}{3}\right) + \left(\frac{\partial\sigma_x^{\kappa}}{\partial x} + \frac{\partial\tau_{xs}^{\kappa}}{\partial s}\right)\left(\frac{\zeta^2}{2}R^2(s) + \frac{2}{3}\zeta^3 R(s) + \frac{\zeta^4}{4}\right)\right\}, \tag{5.44}$$

where $\hat{h}_s(x,s)$ is another function of integration. Dividing eq. 5.44 by $(R(s)+\zeta)^2$ yields

$$\tau_{rs} = \frac{\hat{h}_s(x,s)}{(R(s)+\zeta)^2} -$$
$$\left\{\left(\frac{\partial\sigma_x^{\varepsilon}}{\partial x} + \frac{\partial\tau_{xs}^{\varepsilon}}{\partial s}\right)\left[\frac{\left(R^2(s) + \zeta R(s) + \frac{\zeta^2}{3}\right)\zeta}{(R(s)+\zeta)^2}\right] + \left(\frac{\partial\sigma_x^{\kappa}}{\partial x} + \frac{\partial\tau_{xs}^{\kappa}}{\partial s}\right)\left[\frac{\left(R^2(s) + \frac{4}{3}\zeta R(s) + \frac{\zeta^2}{2}\right)\frac{\zeta^2}{2}}{(R(s)+\zeta)^2}\right]\right\}. \tag{5.45}$$

The terms in square brackets in eq. 5.45 can be simplified due to eq. 5.29. The numerator term in the first square bracket in eq. 5.45 can be written as follows:

$$\left(R^2(s) + \zeta R(s) + \frac{\zeta^2}{3}\right) = R^2(s)\left(1 + \frac{\zeta}{R(s)} + \frac{1}{3}\left(\frac{\zeta}{R(s)}\right)^2\right) \approx R^2(s) \tag{5.46}$$

so

$$\frac{\left(R^2(s) + \zeta R(s) + \frac{\zeta^2}{3}\right)\zeta}{(R(s) + \zeta)^2} \approx \zeta \tag{5.47}$$

Similarly

$$\frac{\left(R^2(s) + \frac{4}{3}\zeta R(s) + \frac{\zeta^2}{2}\right)\frac{\zeta^2}{2}}{(R(s) + \zeta)^2} \approx \frac{\zeta^2}{2}. \tag{5.48}$$

Therefore, eq. 5.45 can be reduced to

$$\begin{aligned} \tau_{rs} &= \frac{\hat{h}_s(x, s)}{(R(s) + \zeta)^2} - \left\{\left(\frac{\partial \sigma_x^{\varepsilon}}{\partial x} + \frac{\partial \tau_{xs}^{\varepsilon}}{\partial s}\right)\zeta + \left(\frac{\partial \sigma_x^{\kappa}}{\partial x} + \frac{\partial \tau_{xs}^{\kappa}}{\partial s}\right)\frac{\zeta^2}{2}\right\} \\ &= h_s(x, s) - \left\{f_s(x, s)\,\zeta + g_s(x, s)\frac{\zeta^2}{2}\right\} \end{aligned} \tag{5.49}$$

where $f_s(x,s)$ and $g_s(x,s)$ are known for each layer at a given value of x and s. The unknown function of integration term has been redefined to be $h_s(x,s)$. The function $h_s^{(k)}(x,s)$ can be determined utilizing the condition that

$$\tau_{rs} = 0 \text{ at } \zeta = -\frac{H}{2} \qquad \left(\text{i. e., } \tau_{rs}^{(1)} = 0 \text{ at } \zeta = -\frac{H}{2}\right) \tag{5.50}$$

and the continuity condition,

$$\tau_{rs}^{(k-1)} = \tau_{rs}^{(k)}, \tag{5.51}$$

where k denotes the layer number. These conditions translate into, respectively,

$$\tau_{rs}^{(1)} = 0 = h_s^{(1)}(x, s) - \left\{f_s^{(1)}(x, s)\left(-\frac{H}{2}\right) + g_s^{(1)}(x, s)\frac{1}{2}\left(-\frac{H}{2}\right)^2\right\} \tag{5.52}$$

or

$$h_s^{(1)}(x, s) = \left\{f_s^{(1)}(x, s)\left(-\frac{H}{2}\right) + g_s^{(1)}(x, s)\frac{1}{2}\left(-\frac{H}{2}\right)^2\right\} \tag{5.53}$$

and

$$h_s^{(k-1)}(x,s) - \left\{ f_s^{(k-1)}(x,s)\zeta_k + g_s^{(k-1)}(x,s)\frac{\zeta_k^2}{2} \right\} = h_s^{(k)}(x,s) - \left\{ f_s^{(k)}(x,s)\zeta_k + g_s^{(k)}(x,s)\frac{\zeta_k^2}{2} \right\} \tag{5.54}$$

or

$$h_s^{(k)}(x,s) = h_s^{(k-1)}(x,s) + (f_s^{(k)}(x,s) - f_s^{(k-1)}(x,s))\zeta_k + (g_s^{(k)}(x,s) - g_s^{(k-1)}(x,s))\frac{\zeta_k^2}{2}, \tag{5.55}$$

for $k = 2, 3, ..., n$.

The interlaminar stresses in principal material coordinate system can be obtained by transformation, namely,

$$\begin{bmatrix} \sigma_{23} \\ \sigma_{13} \end{bmatrix}^k = \begin{bmatrix} \cos\theta_k & -\sin\theta_k \\ \sin\theta_k & \cos\theta_k \end{bmatrix} \begin{bmatrix} \tau_{rs} \\ \tau_{rx} \end{bmatrix}^k. \tag{5.56}$$

It should be noted that the schemes just described for computing the interlaminar stresses do not allow for enforcement of the conditions that the interlaminar shear stresses must be zero at the outer radial location, just as they are at the inner radial location. That is, the conditions

$$\tau_{rx}^{(n)} = \tau_{rs}^{(n)} = 0 \text{ at } \zeta = +\frac{H}{2} \tag{5.57}$$

cannot be explicitly enforced as there are not enough functions of integration $h_x^{(k)}(x,s)$ and $h_s^{(k)}(x,s)$ to allow enforcement. There is, therefore, no guarantee that the conditions of eq. 5.57 will be satisfied. As will be seen, they are not exactly satisfied.

5.3 Character of Interlaminar Stresses

The interlaminar stresses for aluminum and composite circular and elliptical internally pressurized cylinders are illustrated in figs. 5-3 - 5-6 to convey the character of the distribution through the thickness, and to provide some insight into the magnitude of these stresses. These stresses, τ_{rx} and τ_{rs}, or in alternate notation $\tau_{x\zeta}$ and $\tau_{s\zeta}$, are compared at the axial and circumferential locations where the magnitudes of the transverse shear force resultants, Q_x and Q_s, given by eq. 2.7, are maximum. Generally that location is x/L=0.5 and s/C=0 with the exception of the aluminum elliptical cylinder, where the location is x/L=0.5 and s/C=0.15625. These locations are at the end of the cylinder where the condition w=0 is enforced. A review of fig. 2-7, for example, shows the character of $\overline{Q}_x$ and $\overline{Q}_s$ for both circular and elliptical cylinders. Of course the circular cylinder is axisymmetric so the location s/C=0 is not unique.

For the aluminum circular cylinder, fig. 5-3, there is no interlaminar stress τ_{rs}. Note that at ζ=+$H/2$, the shear stress τ_{rx} is not quite zero. As just mentioned, this is due to the lack of enough unknown functions of integration to uniquely specify the shear stress at both ζ=+$H/2$ and ζ=-$H/2$.

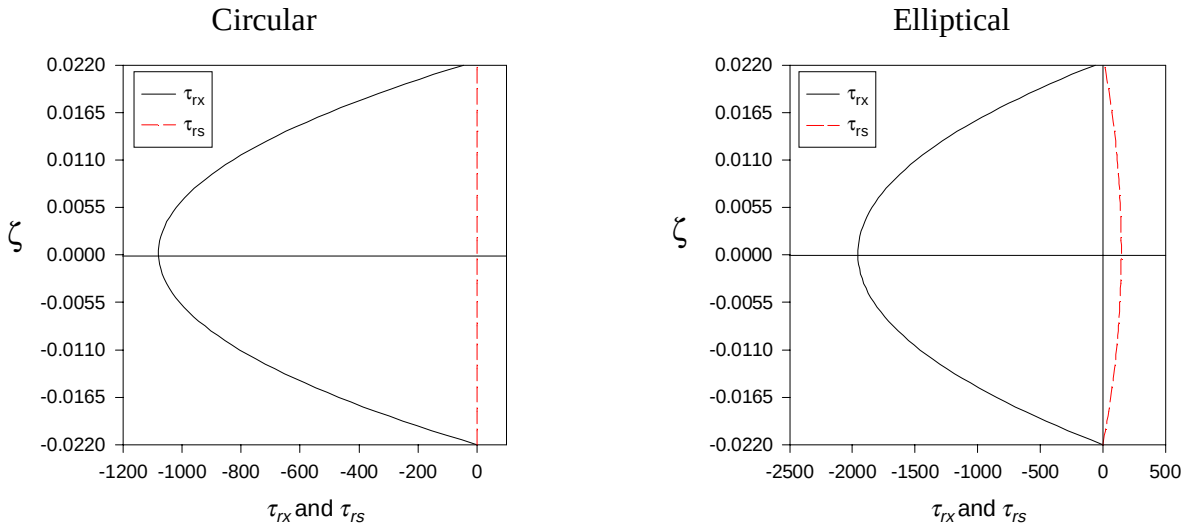

Figure 5-3. Interlaminar shear stresses for an aluminum circular and elliptical cylinders, p_o=100 psi, x/L=0.5, s/C=0.0, except for τ_{rs} for the elliptical cylinder where s/C=0.15625

For the quasi-isotropic cylinder, and the other composite cases, the distributions of the shear stresses are piecewise parabolic, as can be seen from the form of eqs. 5.32 and 5.49. The interlaminar stress τ_{rx} is larger than interlaminar shear stress τ_{rs} and it generally peaks at or near ζ=0. The interlaminar shear stress τ_{rs} generally peaks between the +45° and -45° layers and has a lower value near ζ=0. Note that τ_{rx} is not zero at ζ=+*H/2* and this is felt to be responsible for the lack of symmetry, with respect to ζ=0, of the distribution of the interlaminar shear stresses.

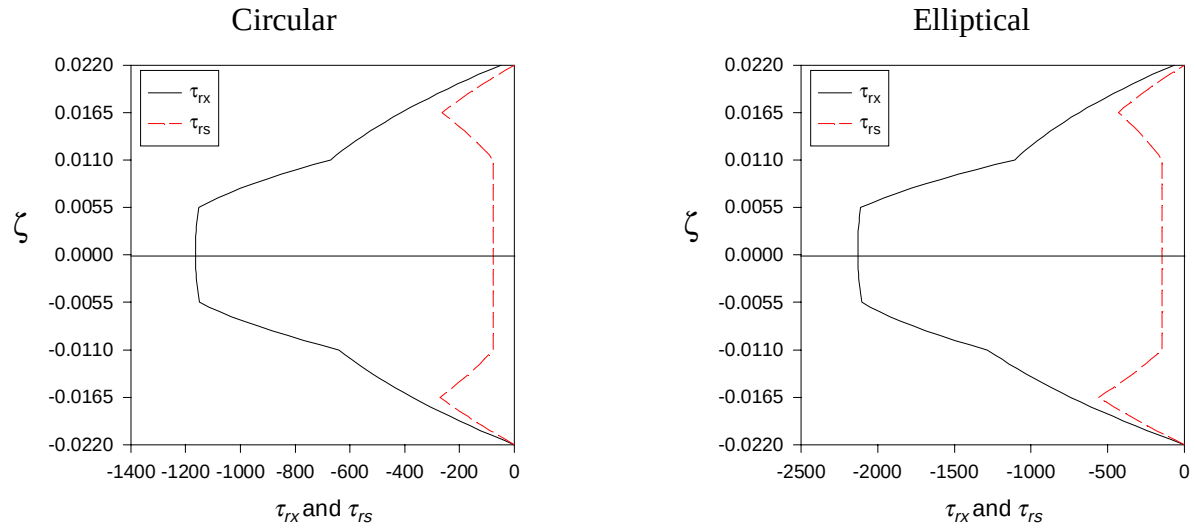

Figure 5-4. Interlaminar shear stresses for a quasi-isotropic circular and elliptical cylinders, p_o=100 psi, x/L=0.5, s/C=0.0

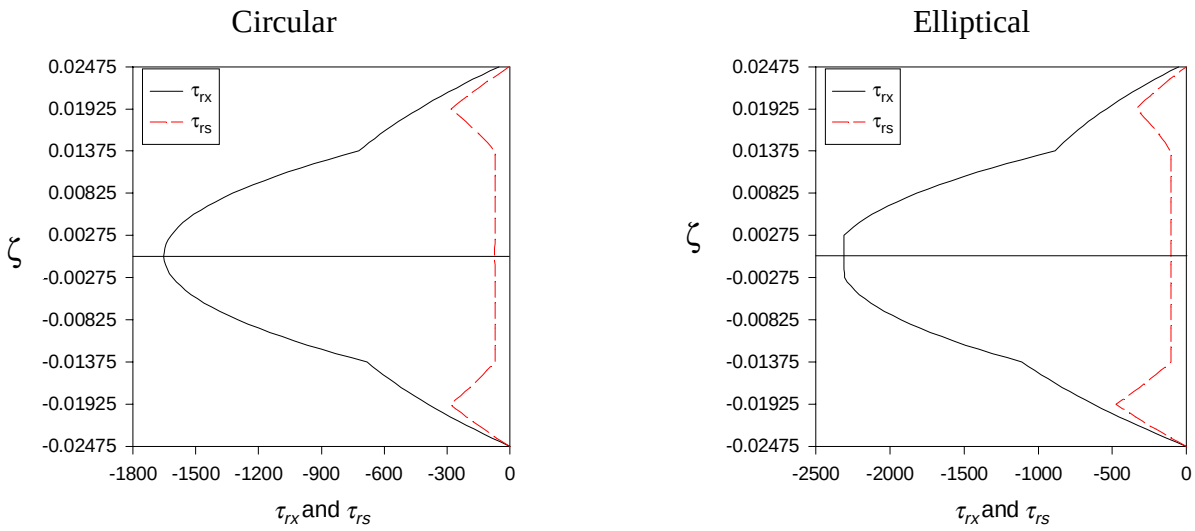

Figure 5-5. Interlaminar shear stresses for an axially-stiff circular and elliptical cylinders, p_o=100 psi, x/L=0.5, s/C=0.0

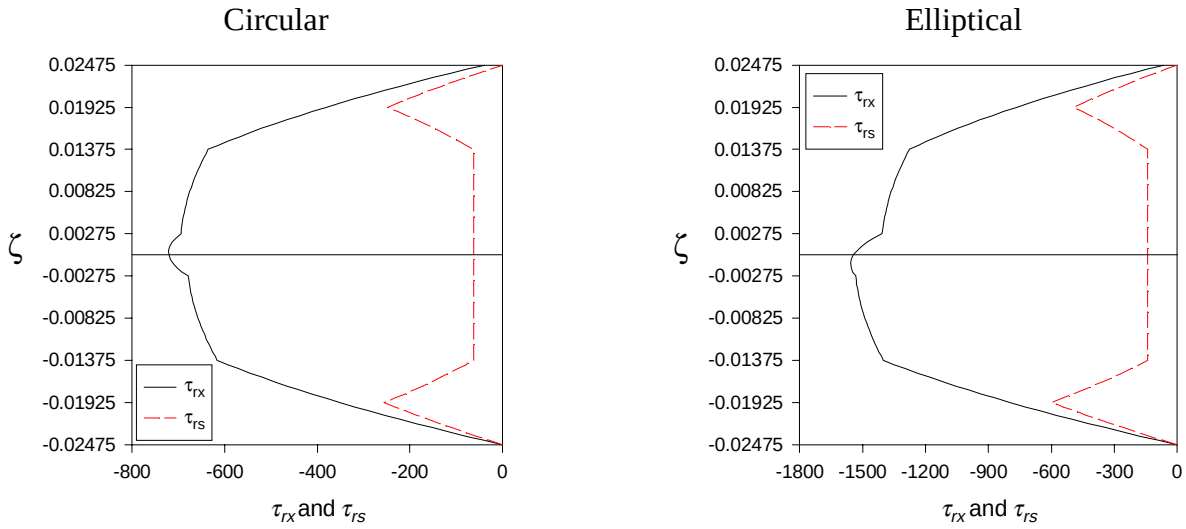

Figure 5-6. Interlaminar shear stresses for a circumferentially-stiff circular and elliptical cylinders, p_o=100 psi, x/L=0.5, s/C=0.0

5.4 Interlaminar Shear Stress Validation

As a check on the interlaminar stress calculations, the integrals of the interlaminar stresses given by eq. 2.7 were compared with the transverse shear stress resultants, Q_x and Q_s, as given by the derivatives of the moments in eq. 2.6. Table 5-1 shows the comparison for the condition of maximum Q_x and the maximum Q_s. In the table the values have been normalized by the quantity p_oR, as has been done earlier, and the *x* and *s* location of the maximum value are indicated, along with the percent error in the integral calculations.

The aluminum circular cylinder does not have a circumferential transverse shear force resultant and the circumferential interlaminar shear stress integrated through the thickness reflects zero response. The integrated axial interlaminar shear stress compared with the axial transverse shear force resultant gives a small error of 3.2%. The aluminum elliptical cylinder shows similar

results for $\int \bar{\tau}_{rx} d\zeta$ and $\overline{Q}_x$, but $\int \bar{\tau}_{rs} d\zeta$ and $\overline{Q}_s$ show a slightly larger error of 7.1%. The composite cylinders also resulted in small differences between the transverse shear force resultants and the integrated interlaminar shear stress. The average error between $\int \bar{\tau}_{rx} d\zeta$ and $\overline{Q}_x$ is 3.5% for the circular composite cylinder and 2.5% for the elliptical composite cylinder. The average error between $\int \bar{\tau}_{rs} d\zeta$ and $\overline{Q}_s$ for both the circular and elliptical composite cylinders is 0.0%. These errors are felt to be minimal.

This chapter has introduced the Hashin and maximum failure criteria, discussed the approach for computing the inplane stresses, and presented a method for computing the interlaminar shear stresses that contribute to the failure criteria. The integral of the interlaminar shear stresses through the thickness were compared to the transverse shear stress resultant to verify the derivation of the interlaminar shear stresses. The difference between the integrated interlaminar shear stresses and the transverse shear stress resultant was considered to be negligible.

Table 5-1. Linear interlaminar shear stress comparison

		Aluminum	Quasi-isotropic	Axially-stiff	Circumferen-tially-stiff
Circular	$\overline{Q}_x$	0.06203	0.06035	0.08843	0.05050
	$\int \bar{\tau}_{rx} d\zeta$	0.06402	0.06252	0.09092	0.05247
	% Error	3.2	3.6	2.8	3.9
	Location (*x/L*,s/*C*)	(0.5,0.0)	(0.5,0.0)	(0.5,0.0)	(0.5,0.0)
	$\overline{Q}_s$	0	0.01010	0.01084	0.00970
	$\int \bar{\tau}_{rs} d\zeta$	0	0.01010	0.01085	0.00970
	% Error	0	0.0	0.0	0.0
	Location (*x/L*,s/*C*)	(0.5,0.0)	(0.5,0.0)	(0.5,0.0)	(0.5,0.0)
Elliptical	$\overline{Q}_x$	0.11291	0.11104	0.12662	0.10889
	$\int \bar{\tau}_{rx} d\zeta$	0.11564	0.11406	0.12921	0.11216
	% Error	2.4	2.7	2.0	3.0
	Location (*x/L*,s/*C*)	(0.5,0.0)	(0.5,0.0)	(0.5,0.0)	(0.5,0.0)
	$\overline{Q}_s$	0.00820	0.01894	0.01593	0.02138
	$\int \bar{\tau}_{rs} d\zeta$	0.00878	0.01895	0.01593	0.02140
	% Error	7.1	0.0	0.0	0.0
	Location (*x/L*,s/*C*)	(0.5,0.15625)	(0.5,0.0)	(0.5,0.0)	(0.5,0.0)